A Numerical Investigation of TBA.....!!!1

By H.G.K.G Jayatunga

Contents

CHAPTER 1

A REVIEW OF THE LITERATURE

1.1 Flow induced vibrations

1.2 Fluid-elastic galloping

Fluid-elastic galloping is one of the most commonly observable flow-induced vibration on a slender body. Since this phenomenon is most common in civil structure, such as buildings and iced-transmission lines, the term "aeroelastic galloping" is commonly used as the body is immersed in air. However, this mechanism can occur on a slender body immersed in any Newtonian fluid, provided that the conditions to sustain the galloping mechanism are satisfied. This work is based on a general Newtonian flow,thus the term " fluid-elastic galloping" is used throughout this thesis.

1.2.1 Excitation of galloping

Païdoussis et al. (2010) describes galloping as a "velocity dependent and damping controlled" phenomenon. Therefore, in order for a body to gallop, an initial excitation has to be given to that body. While this excitation is mainly caused by the force crated from vortex shedding, other fluid instabilities may contribute to this initial excitation. When a bluff body moves along the transverse direction of the fluid flow, it generates a force along the transverse direction. This force, also known as the induced lift is a resultant of the velocity of the fluid and the motion of the body. When this body is attached to an
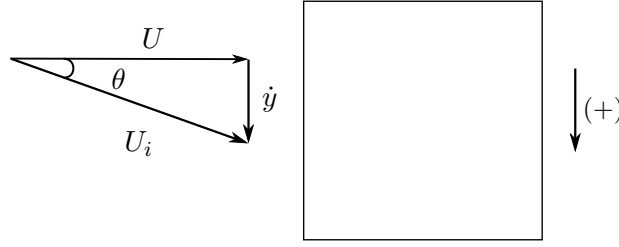
Figure 1.1: Induced angle of attack on the square prism due to the resultant of free-stream velocity of the fluid and transverse velocity of the body.

oscillating system (i.e. a simple spring, mass and damper system), the induced lift becomes the periodic forcing of the system. Galloping is sustained if the induced lift is in phase with the motion of the body. This could be explained further by using a square cross section as an example.

Figure 1.1 illustrates the motion of the body at a given instantaneous time.The induced angle of attack is formed on the square cross section as a result of the fressrteam velocity vector U and the transverse velocity vector of the body $\dot{y}$. Thus, a force is formed in phase with the motion of the body (square cross section). This mechanism could also be observed on other bodies which are prone to galloping. The sign convention in this figure (and generally used in this scope of research) states that downward direction is positive. Hence, the force generated on a body under the influence of galloping, could be also identified as a "negative lift".

1.2.2 Quasi-steady state theory

According Païdoussis et al. (2010),the initial studies by Glauert (1919) provided a criterion for galloping by considering the auto-rotation of a stalled aerofoil. As this phenomenon commonly occur in iced transmission lines, Den Hartog (1956) has provided a theoretical explanation for iced electric transmission lines.

The pioneering study in order to mathematically model galloping was conducted by Parkinson and Smith (1964). This model has been widely used in almost all subsequent studies regarding galloping. A weakly non-linear oscillator model was developed by them to predict the response of the system. Essentially the quasi-steady assumption was made to develop this theory assuming that the instantaneous induced lift force of the oscillating

body is equal to that of the lift force generated by the same body at the same induced angle of attack. In order to satisfy the quasi-steady assumption few conditions had to be satisfied.

- The velocity of the body does not change rapidly

- There is no interaction between vortex shedding and galloping

The second condition is satisfied by ensuring the vortex shedding frequency is much higher than the galloping frequency. The oscillator equation was solved using the Krylov and Bogoliubov method. Details of this method would not be mentioned as it is not used in the present study to solve the oscillator equation. The results obtained form experiments, carried out at $Re = 2200$ and a mass ratio (m^*) around 1164 had a good agreement with the theoretical data which is shown in figure 1.2.

Quasi-steady state oscillator model

The equation of motion of transversely oscillating body is given by

$$m\ddot{y} + c\dot{y} + ky = F_y, \tag{1.1}$$

where the forcing term F_y is given by

$$F_y = \frac{1}{2}\rho U^2 \mathcal{A} C_y. \tag{1.2}$$

As explained previously, when quasi-steady assumption is used the stationary C_y data (which consists of both lift and drag data) of the body could be could be used as inputs to the oscillator equation.Parkinson and Smith (1964) used a 7th order odd interpolating polynomial to determine C_y. The order of the polynomial can be chosen arbitrarily depending on the study. For example Barrero-Gil et al. (2009, 2010) have used a 3_{rd} order polynomial in order to simplify the analytical model. However, Ng et al. (2005) pointed out that a 7_{th} order polynomial is sufficient as it does not provide a significantly better result.

$$C_y(\theta) = a_1 \left(\frac{\dot{y}}{U}\right) - a_3 \left(\frac{\dot{y}}{U}\right)^3 + a_5 \left(\frac{\dot{y}}{U}\right)^5 - a_7 \left(\frac{\dot{y}}{U}\right)^7. \tag{1.3}$$
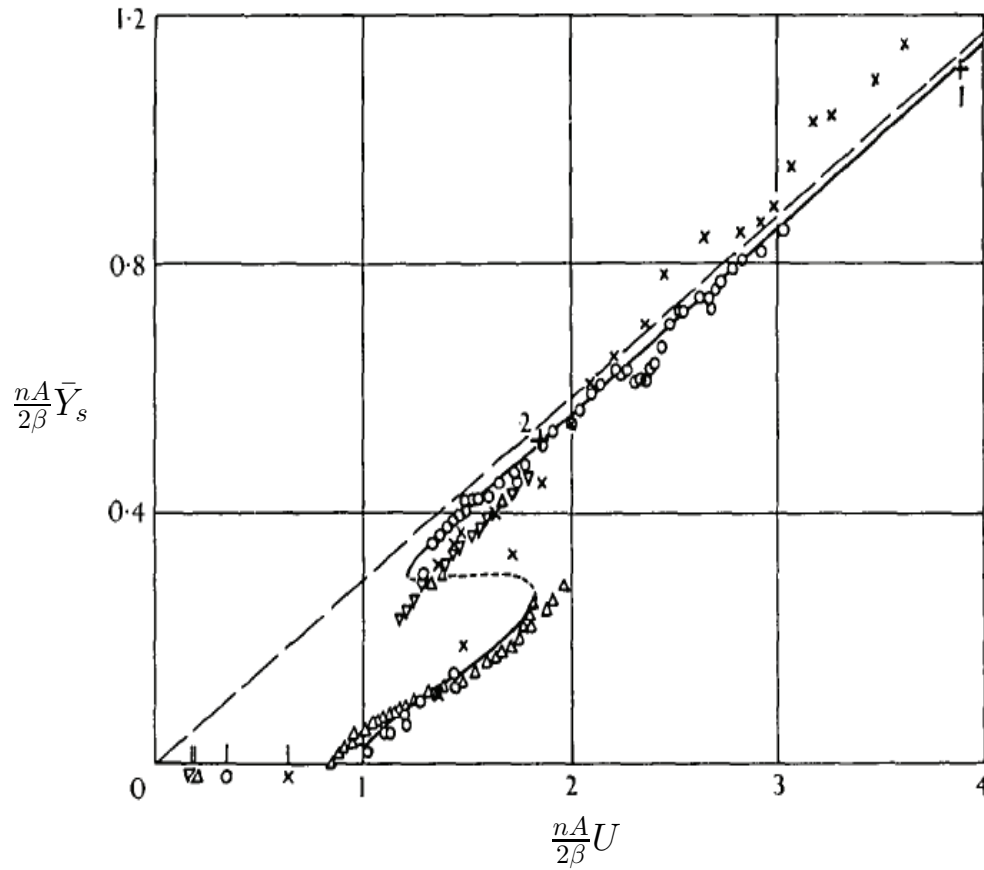
Figure 1.2: "Collapsed amplitude-velocity characteristic. Theory: ——— stable limit cycle, - - - unstable limit cycle. Experiment $\times$ $\beta = .00107$, $\circ$ $\beta = .00196$, $\triangle$ $\beta = .00364$, $\triangledown$ $\beta = .00372$, $+1$ $\beta = .0012$, $+2$ $\beta = .0032$ Reynolds numbers $4,000 - 20,000$ ". Figure extracted from Parkinson and Smith (1964). $\frac{nA}{2\beta}\bar{Y}_s$ is the dimensionless displacement amplitude parameter and $\frac{nA}{2\beta}U$ is the reduced velocity.

Therefore by substituting the forcing function to the oscillator equation (Eq:1.1) the Quasi-steady state (QSS) model could be obtained (Eq:1.4).

$$m\ddot{y}+c\dot{y}+ky=\frac{1}{2}\rho U^2\mathcal{A}\left(a_1\left(\frac{\dot{y}}{U}\right)-a_3\left(\frac{\dot{y}}{U}\right)^3+a_5\left(\frac{\dot{y}}{U}\right)^5-a_7\left(\frac{\dot{y}}{U}\right)^7\right). \qquad (1.4)$$

As the current study is focused on the low Re region, it is a known fact that the vortex shedding will be correlated well and therefore provide a significant forcing in the low Reynolds number region. Joly et al. (2012) introduced and additional sinusoidal forcing function to the model in order to integrate the forcing by vortex shedding. By the addition of this forcing Joly et al. (2012) managed to obtain accurate predictions of the displacement amplitude even at low mass ratios, where the galloping is suppressed or not present. Yet, the strength or the amplitude of this sinusoidal forcing has to be tuned in an *ad hoc* manner, and it was not clear the relationship between this forcing with the other system parameters. Thus in the current study this forcing was not used.

Presence of hysteresis

Hysteresis could be observed in the in the amplitude data of Parkinson and Smith (1964). In contrast, the studies carried out by Barrero-Gil et al. (2009) and Joly et al. (2012) at much lower Reynolds numbers ($159 \leq Re \leq 200$), did not show any hysteresis. Luo et al. (2003) concluded that the hysteresis was present due to the presence of an inflection point in the C_y curve at high Reynolds numbers (Parkinson and Smith (1964) data) which was not present at lower Reynolds numbers. It was further explained and demonstrated by Luo that the inflection point occurs due to the intermittent re attachment of the shear layer in certain angles at high Reynolds numbers.

1.2.3   Induced force and the shear layers

It is important to have an understanding on how the induced lift is generated in a fluid dynamics point of view. The quasi-steady model has already been validated and re-validated by many studies, therefore the flow-field data of static body simulations could be used to analyse the underpinning fluid dynamic mechanisms governing galloping.

The governing mechanism of galloping is the behaviour of the shear layers created at the leading edge due to flow separation on the top and bottom of the body. A common
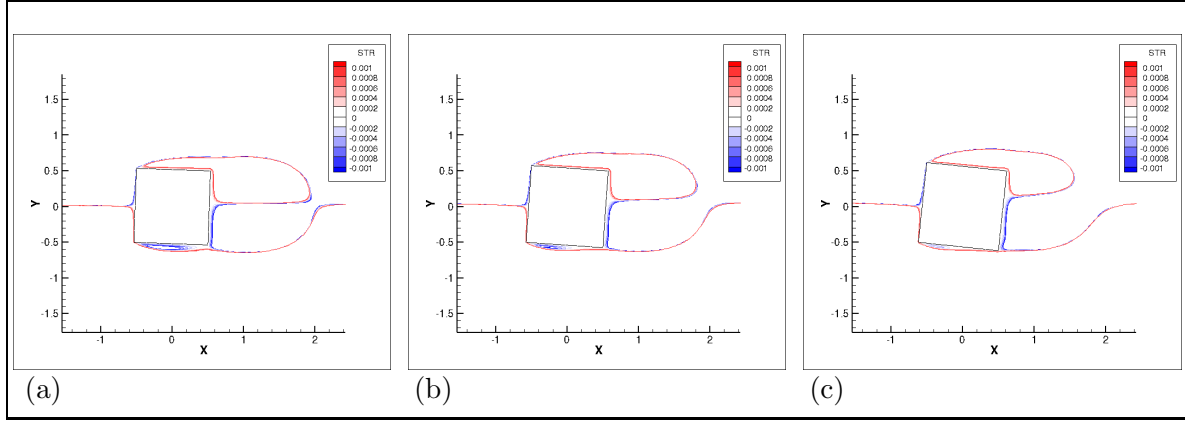
Figure 1.3: Stream functions of time averaged flow field on a stationary square section at $Re = 200$ at different incidence angles. (a) $2°$ (C_y increases),(b) $4°$ (C_y peaks) and (c) $2°$ (C_y decreases). The bottom shear layer comes closer to the bottom wall and reattaches as the angle of incidence increase.

example is a square cross section which has been used widely in studies on galloping. In this square cross section (figure 1.3) the flow separate from the leading edges of the body and create two shear layers on the top and bottom sides of the the body. Figure 1.3 shows the stream functions of time averaged (over a vortex shedding cycle) flow fields of stationary cross sections. The angle of incidence increases clockwise from $2° - 6°$. As θ is increased, the bottom shear comes closer to the wall of the body compared to the top shear layer (Figure 1.3 (a)). The shear layer nearer to the body crates higher suction compared to the shear layer at the opposite side. This pressure imbalance between the top and bottom sides of the body creates a downward force (i.e. the negative lift). As the angle is increased, the bottom shear layer becomes more closer and therefore the pressure difference becomes grater leading to a higher C_y. The negative lift force becomes maximum when the shear layer near to the wall reattaches at the trailing edge (figure 1.3 (b)). As θ is further increased, the bubble in the bottom shear layer shrinks in size resulting the reduction of the pressure imbalance of the top and bottom surface leading to the reduction in C_y. put the cY curve as crodd reference . As the body is connected to an oscillatory system (discussed in section 1.2.1), this shear layer behaviour also harmonize with the cyclic behaviour of the system providing the driving force to the system so that the motion of galloping is sustained.

1.2.4 Frequency response

It is clear that the cyclic motion of the shear layer harmonize with the mechanical system. Therefore, the frequency response should be then, the natural frequency of the system ω_n which much is different from VIV mechanism, where the primary frequency comes from the periodic forcing of the vortex shedding. Hence, in the QSS model the natural frequency of the system could be identified as the frequency of oscillations. However, it should be noted that this is valid on the regimes where the conditions discussed in section 1.2.2 are satisfied.

On the other hand, the forcing function in the QSS model equation 1.4, is a non linear function. As the mass ratio is quite high, the non-linearities of the forcing does not make much effect to the frequency response. However, as the mass ratio goes down theoretically the non linearities of the forcing should affect the frequency response of the system.

The experimental studies carried by Bouclin (1977) concluded at high reduced velocities with large inertia, the motion of the cylinder controls the frequency of the system rather than the vortex shedding. The structural damping has no effect provided that it is small. He also concluded that as the inertia and the reduced velocity gets lower, there is some interaction between vortex shedding and galloping. And at this region the frequency is mainly governed by the vortex shedding.

1.2.5 Fluid mechanics governing the galloping response

As discussed in subsection 1.2.3 the driving force of a galloping system is the asymmetrical placement of the shear layers at either sides of the body. In consequence, it is clear that a significant afterbody is needed for the shear layer interaction to sustain galloping. Parkinson (1974, 1989) and Bearman et al. (1987) have discussed well the importance of the length and the shape for galling in their reviews. It is also highlighted in Parkinson (1974) that the most important physical parameters for galloping are the size relative to the characteristic hight and the shape of the afterbody. Manipulating the shape of the afterbody and thereby, manipulating the shear layer interactions with the body, gives the ability to control the galloping response. Thus, due to this reason work has been carried out on the response of galloping of different cross sectional shapes.

Blevins (1990) provided a good comparison of the shapes which are prone to galloping based on the work by Parkinson and Brooks (1961), Nakamura and Mizota (1975) and Nakamura and Tomonari (1977). The reproduction of Blevins's data could be found in Païdoussis et al. (2010) presented in figure 1.4.
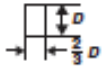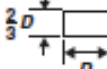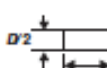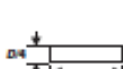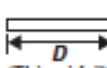
Naudascher and Wang (1993), Ruscheweyh et al. (1996), Deniz (1997) and Weaver and Veljkovic (2005) are some of the work done on different cross sectional shapes. Alonso et al. (2009) carried out wind tunnel tests on biconvex and rhomboidal cross sections. Studies were further carried out by Alonso for elliptical cross sections (Alonso et al., 2010) and triangular cross sections (Alonso et al., 2005). The regions of stability for galloping at different angles of attack and the static force coefficients are presented in these studies with regards to the cross section involved.

1.2.6 Galloping as a mechanism of energy harvesting

The focus on fluid-elastic galloping in the past was on understanding and developing methods to suppress it, due to the adverse effects on civil structures. However, recently, the focus of research has been redirected to develop mechanisms to excite galloping rather than suppressing it. This is due to the recent trend on the search of alternate energy sources with minimal environmental impact have lead researchers working on investigating the possibility of extracting useful energy from flow induced vibrations.

Bernitsas and his group in the University of Michigan have made significant progress on using VIV as potential candidate for energy extraction. Bernitsas et al. (2008) introduced the concep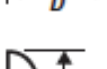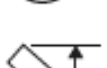t of using VIV as a mode of energy extraction.The group have developed a device called VIVACE converter based on this concept. The work has been further expanded to focus on various aspects (such as Reynolds number effects, damping effects etc.) in Bernitsas et al. (2009); Raghavan et al. (2009); Raghavan and Bernitsas (2011); Lee et al. (2011).

To this end, investigations on the possibility of using fluid-elastic galloping as a mode of energy extraction have not being pursued much. Barrero-Gil et al. (2010) was the first work which placed the concept of using fluid-elastic galloping as a mode of energy harvesting. In his paper Barrero-Gil et al. (2010) clearly explains the advantages of using galloping as a mode of energy harvesting. Unlike VIV, galloping is not a resonant phenomenon which

Section	h/d	$\partial C_{F_y}/\partial\alpha$ Smooth flow	$\partial C_{F_y}/\partial\alpha$ Turbulent flow[b]	Reynolds number
(square, $D \times D$)	1	3.0	3.5	10^5
(rectangle, D high, $\frac{2}{3}D$ wide)	3/2	0.	−0.7	10^5
(rectangle, D high, $D/2$ wide)	2	−0.5	0.2	10^5
(rectangle, D high, $D/4$ wide)	4	−0.15	0.	10^5
(rectangle, $\frac{2}{3}D$ high, D wide)	2/3	1.3	1.2	6.6×10^4
(rectangle, $D/2$ high, D wide)	1/2	2.8	−2.0	3.3×10^4
(rectangle, $D/4$ high, D wide)	1/4	−10.	–	$2 \times 10^3 - 2 \times 10^4$
(Thin airfoil, width D)	–[c]	−6.3	−6.3	$> 10^3$
(airfoil, D)	–	−6.3	−6.3	$> 10^3$
(D-section, D)	–	−0.1	0.	6.6×10^4
(half-circle)	–	−0.5	2.9	5.1×10^4
(angle section, D)	–	0.66	–	7.5×10^4

[a] α is in radians; flow is left to right. $\partial C_{F_y}/\partial\alpha = -\partial C_L/\partial\alpha - C_D$, with C_{F_y} based on the dimension D, so that $\partial C_{F_y}/\partial\alpha > 0$ for galloping.
[b] Approximately 10% turbulence.
[c] Inappropriate to use h/d.

Figure 1.4: "The transverse force coefficient for various sections in steady smooth or turbulent flow (after Blevins (1990))" obtained from Païdoussis et al. (2010)

needs the synchronisation or "lock-in" and therefore have the following advantages.

- The range where significant oscillations develop is not restricted to a narrow band of frequencies.

- Galloping does not have a self-limited response beyond the critical velocity (Barrero-Gil et al., 2010) and therefore the amplitudes increase as the flow velocity is increased.

CHAPTER 2

METHODOLOGY AND VALIDATION

2.1 Introduction

A brief overview of the computational methods to perform the simulations to obtain the data in this thesis are are presented in this chapter. As the this particular study is not focused on developing computational methods but concentrated on understanding the physics of a body under the influence of fluid-elastic galloping, it should be noted that the overview provided in this chapter is quite abstract.

The flow of this chapter is as follows. First the equations used to model the system are presented and

Finally, a series of validation data are presented and discussed to ensure the accuracy of the direct numerical simulations in order to ensure the confidence in the numerical predictions of this thesis.

2.1.1 Parameters used

The data in this project are mainly presented in two categories, high and low Reynolds numbers to compare results at laminar and turbulent range. One main objectives in this study was to capture the flow physics accurately using direct numerical simulations hence,major portion of the study was carried out in the laminar range where the flow is close to 2D. Although majority of data are focused on low Reynolds numbers, some data were presented using inputs from high Reynolds numbers to the QSS model to provide a comparison between high and low Reynolds numbers. $Re = 200$ was defined as the "low" Reynolds

number and $Re = 22300$ was defined as the high Reynolds number. Studies by Tong et al. (2008) and Sheard et al. (2009) reveals that the approximate value of 3-dimensional transition of the wake for a square cross section is $Re = 160$ and therefore, $Re = 200$ was selected to represent the low Reynolds number regime, also considering the fact that other numerical studies in the laminar regime have used this value for the Reynolds number (Robertson et al., 2003; Joly et al., 2012). The reason behind considering the flow regimes of a square cross section was the fact that the basic cross section being used in this study was a square. The selection of the value for the high Reynolds number was fairly was simple as it was the Reynolds number where the pioneering study of galloping Parkinson and Smith (1964) provided the experimental input data ($C_y data$) for the QSS model.

Stationary C_y data at different angles of attack to be used as inputs to the QSS model, were obtained for the low Reynolds number regime using direct numerical simulations. The average power was obtained by using equation 2.1, and the averaging was done over no less than 20 galloping periods. For the high Re tests, predictions of power output at $Re = 22300$ were obtained using the coefficients for the C_y curve from Parkinson and Smith (1964). The mass ratio m^* was kept at 1163 for $Re = 22300$ (Similar to Parkinson and Smith (1964)), $m^* = 20$ for Re=200 and $U^* \geq 40$ similar to the parameters used in literature (Robertson et al., 2003; Joly et al., 2012) to obtain a comparison with published work. These parameters were used throughout this study unless otherwise specified.

2.2 Quasi-steady model

The quasi-steady state model discussed in section 1.2.2 was used to obtain oscillator response data. The quasi-steady state model has proven its ability to obtain accurate galloping response data (discussed in section 1.2.2). Therefore, it enables to obtain large number of at the expense of a short computational time. The oscillator equation consist of spring, mass and damper oscillator expression with a 7th order interpolation polynomial as the forcing function (equation 1.4).

Solving the quasi-steady state equation

The quasi-steady model being an ordinary differential equation could be solved using different solving methods. Some of the techniques include limit cycle oscillations, harmonic balance, cell mapping and numerical integration. Vio et al. (2007) showed that numerical integration provides accurate data. A fourth-order Runge-Kutta ODE solving scheme was used in solving the quasi-steady state oscillator equation. The built in 'ode45' function in MATLAB was used primarily to solve the QSS equation while in some cases 'ode15s' function was used when the equation became more stiff.

2.3 Calculation of average power

The ideal potential amount of harvested power output could be represented as the dissipated power due to mechanical damping before losses in any power take-off system are included. Thus the mean power output could be expressed as

$$P_m = \frac{1}{T} \int_0^T (c\dot{y})\dot{y}dt, \tag{2.1}$$

where T is the period of integration and c is the mechanical damping constant.

The work done on the body by the fluid is equal to this quantity, defined as

$$P_m = \frac{1}{T} \int_0^T F_y\dot{y}dt, \tag{2.2}$$

where F_y is the transverse (lift) force.

The two definitions of the mean power provide two vital interpretations of power transfer. Equation 2.1 shows that the power is proportional to the mechanical damping and the magnitude of the transverse velocity. At first glance one may assume that the power could be increased by increasing damping. In a practical power extraction device, the significant component of damping would be due to the electrical generator and therefore, an increase in damping would be due to the increase of the load or in other words the electrical resistance. Yet this perception of damping is not quite accurate as very high damping would result in reducing the velocity amplitude which then, would not result in a higher energy output according to equation 2.1. In consequence, a balance need to be obtained where the

damping is high, but not to the extent that it will adversely result by overly suppressing the motion of the body.

On the other hand, equation 2.2 shows that a higher power is attained during situations where the transverse force F_y and the transverse velocity are in phase. Hence, a simple increase in the magnitude of the force or the velocity is not satisfactory to attain a higher power transfer. Any increase in magnitude of either of the parameters (force or velocity) is linked to an increase in phase.

Direct numerical simulations (DNS)

Direct numerical simulations were employed to obtain the stationary data to be used as inputs to the QSS model and to obtain fluid-structure interaction (FSI) data to be compared with the QSS model at low Reynolds numbers. A high-order in-house build spectral element which simulates two-dimensional laminar flows was used to obtain the DNS data.

Boundary conditions

The boundary conditions, regardless of the mesh were common for all the simulations performed. A no-slip condition was applied to the cross section wall. This condition implied that the velocity is zero at the surface of the cross section. For stationary simulations a Dirichlet boundary condition and for FSI cases a time-dependent Dirichlet boundary condition was employed for the velocity on the inlet and lateral boundaries. A Dirichlet boundary condition should have a specified value for the variables (Kreyszig, 2010) in this case velocity. The time-dependent Dirichlet condition has to be implemented for the FSI cases to account for the accelerated reference frame attached to the cross section. Thus, the inlet boundary was set to $u = U$ and $v = -\dot{y}$ for FSI cases and $v = 0$ for stationary cases, where u, v are the velocities in the x and y directions, respectively.

A Neumann condition for the pressure (where the gradient of a property is specified Tu et al. (2008)), where the normal gradient was calculated from the Navier–Stokes equations, was employed on the inlet, lateral and body surface (Gresho and Sani, 1987), while a Dirichlet condition for the pressure ($p = 0$ was enforced at the outlet. The details of the method can be found in Thompson et al. (2006, 1996)

Although the physical validity of the outlet boundary condition is not quite true, this

does not turn out to be a significant problem provided that the Reynolds numbers are low and the domain is sufficiently far away from the body.

Solving method

and a description of the spectral element method in general can be found in Karniadakis and Sherwin (2005). This code has been very well validated in a variety of fluid-structure interaction problems similar to that studied in this paper (Leontini et al., 2007; Griffith et al., 2011; Leontini et al., 2011; Leontini and Thompson, 2013).

Bibliography

Alonso, G., Meseguer, J., Pérez-Grande, I., 2005. Galloping instabilities of two-dimensional triangular cross-section bodies. Experiments in Fluids 38, 789–795.

Alonso, G., Meseguer, J., Sanz-Andrés, A., Valero, E., 2010. On the galloping instability of two-dimensional bodies having elliptical cross-sections. Journal of Wind Engineering and Industrial Aerodynamics 38, 789–795.

Alonso, G., Valero, E., Meseguer, J., 2009. An analysis on the dependence on cross section geometry of galloping stability of two-dimensional bodies having either biconvex or rhomboidal cross sections. European Journal of Mechanics B/Fluids 28, 328–334.

Barrero-Gil, A., Alonso, G., Sanz-Andres, A., Jul. 2010. Energy harvesting from transverse galloping. Journal of Sound and Vibration 329 (14), 2873–2883.

Barrero-Gil, A., Sanz-Andrés, A., Roura, M., Oct. 2009. Transverse galloping at low Reynolds numbers. Journal of Fluids and Structures 25 (7), 1236–1242.

Bearman, P. W., Gartshore, I. S., Maull, D. J., Parkinson, G. V., 1987. Experiments on f low-induced vibration of a square-section cylinder. Journal of Fluids and Structures 1, 19–34.

Bernitsas, M. M., Ben-Simon, Y., Raghavan, K., Garcia, E. M. H., 2009. The VIVACE Converter: Model Tests at High Damping and Reynolds Number Around 10[sup 5]. Journal of Offshore Mechanics and Arctic Engineering 131 (1), 011102.

Bernitsas, M. M., Raghavan, K., Ben-Simon, Y., Garcia, E. M. H., 2008. VIVACE (Vortex Induced Vibration Aquatic Clean Energy): A new concept in generation of clean and

renewable energy from fluid flow. Journal of Offshore Mechanics and Arctic Engineering 130 (4), 041101–15.

Blevins, R. D., 1990. Flow-Induced Vibration, 2nd Edition. New York: Van Nostrand Reinhold.

Bouclin, D. N., 1977. Hydroelastic oscillations of square cylinders. Master's thesis, University of British Columbia.

Den Hartog, J. P., 1956. Mechanical Vibrations. Dover Books on Engineering. Dover Publications.

Deniz, S. amd Staubli, T., 1997. Oscillating rectangular and octagonal profiles: Interaction of leading-and trailing-edge vortex formation. Journal of Fluids and Structures 11, 3–31.

Glauert, H., 1919. The rotation of an aerofoil about a fixed axis. Tech. rep., Advisory Committee on Aeronautics R and M 595. HMSO, London.

Gresho, P. M., Sani, R. L., 1987. On pressure boundary conditions for the incompressible Navier–Stokes equations. International journal for numerical methods in fluids 7, 1111–1145.

Griffith, M. D., Leontini, J. S., Thompson, M. C., Hourigan, K., 2011. Vortex shedding and three-dimensional behaviour of flow past a cylinder confined in a channel. Journal of Fluids and Structures 27 (5-6), 855–860.

Joly, A., Etienne, S., Pelletier, D., Jan. 2012. Galloping of square cylinders in cross-flow at low Reynolds numbers. Journal of Fluids and Structures 28, 232–243.

Karniadakis, G. E., Sherwin, S., 2005. Spectral/hp element methods for computational fluid dynamics, ii Edition. Oxford University.

Kreyszig, E., 2010. Advanced Engineering Mathematics, 10th Edition. John Wiley & Sons.

Lee, J., Xiros, N., Bernitsas, M., Apr. 2011. Virtual damperspring system for VIV experiments and hydrokinetic energy conversion. Ocean Engineering 38 (5-6), 732–747.

Leontini, J. S., Lo Jacono, D., Thompson, M. C., Nov. 2011. A numerical study of an inline oscillating cylinder in a free stream. Journal of Fluid Mechanics 688, 551–568.

Leontini, J. S., Thompson, M. C., 2013. Vortex-induced vibrations of a diamond cross-section: Sensitivity to corner sharpness. Journal of Fluids and Structures 39, 371–390.

Leontini, J. S., Thompson, M. C., Hourigan, K., Apr. 2007. Three-dimensional transition in the wake of a transversely oscillating cylinder. Journal of Fluid Mechanics 577, 79.

Luo, S., Chew, Y., Ng, Y., Aug. 2003. Hysteresis phenomenon in the galloping oscillation of a square cylinder. Journal of Fluids and Structures 18 (1), 103–118.

Nakamura, Y., Mizota, T., 1975. Unsteady lifts and wakes of oscillating rectangular prisms. ASCE Journal of the Engineering Mechanics Division 101, 855–871.

Nakamura, Y., Tomonari, Y., 1977. Galloping of rectangular prisms in a smooth and in a turbulent flow. Journal of Sound and Vibration 52, 233–241.

Naudascher, E., Wang, Y., 1993. Flow induced vibrations of prismatic bodies and grids of prisms. Journal of fluids and structures 7, 341–373.

Ng, Y., Luo, S., Chew, Y., Jan. 2005. On using high-order polynomial curve fits in the quasi-steady theory for square-cylinder galloping. Journal of Fluids and Structures 20 (1), 141–146.

Païdoussis, M., Price, S., de Langre, E., 2010. Fluid-Structure Interactions : Cross-Flow-Induced Instabilities. Cambridge University Press.

Parkinson, G., 1989. Phenomena and modelling of flow-induced vibrations of bluff bodies. Progress in Aerospace Sciences 26, 169–224.

Parkinson, G., Brooks, N. P. H., 1961. On the aeroelastic instability of bluff cylinders. Journal of Applied Mechanics 28, 252–258.

Parkinson, G. V., 1974. Mathematical models of flow-induced vibrations of bluff bodies. In Flow-Induced Structural Vibrations, e. naudascher Edition. Berlin: SpringerVerlag.

Parkinson, G. V., Smith, J. D., 1964. The square prism as an aeroelastic non-linear oscillator. The Quarterly Journal of Mechanics and Applied Mathematics 17 (2), 225–239.

Raghavan, K., Bernitsas, M., Apr. 2011. Experimental investigation of Reynolds number effect on vortex induced vibration of rigid circular cylinder on elastic supports. Ocean Engineering 38 (5-6), 719–731.

Raghavan, K., Bernitsas, M. M., Maroulis, D. E., 2009. Effect of Bottom Boundary on VIV for Energy Harnessing at $8 \times 10^3 < Re < 1.5 \times 10^5$. Journal of Offshore Mechanics and Arctic Engineering 131 (3), 031102.

Robertson, I., Li, L., Sherwin, S. J., Bearman, P. W., 2003. A numerical study of rotational and transverse galloping rectangular bodies. Journal of Fluids and Structures 17, 681 – 699.

Ruscheweyh, H., Hortmanns, M., Schnakenberg, C., 1996. Vortex-excited vibrations and galloping of slender elements. Journal of Wind Egineering and Industrial Aerodynamics 65, 347–352.

Sheard, G. J., Fitxgerald, M. J., Ryan, K., Jun. 2009. Cylinders with square cross-section: wake instabilities with incidence angle variation. Journal of Fluid Mechanics 630, 43.

Thompson, M., Hourigan, K., Sheridan, J., Feb. 1996. Three-dimensional instabilities in the wake of a circular cylinder. Experimental Thermal and Fluid Science 12 (2), 190–196.

Thompson, M. C., Hourigan, K., Cheung, A., Leweke, T., Nov. 2006. Hydrodynamics of a particle impact on a wall. Applied Mathematical Modelling 30 (11), 1356–1369.

Tong, X., Luo, S., Khoo, B., Oct. 2008. Transition phenomena in the wake of an inclined square cylinder. Journal of Fluids and Structures 24 (7), 994–1005.

Tu, J., Yeoh, G., Liu, C., 2008. Computational Fluid Dynamics: A Practical Approach, 1st Edition. Butterworth-Heinemann.

Vio, G., Dimitriadis, G., Cooper, J., Oct. 2007. Bifurcation analysis and limit cycle oscillation amplitude prediction methods applied to the aeroelastic galloping problem. Journal of Fluids and Structures 23 (7), 983–1011.

Weaver, D. S., Veljkovic, I., 2005. Vortex shedding and galloping of open semi-circular and parabolic cylinders in cross-flow. Journal of Fluids and Structures 21, 65–74.